



# SEISMIC LIFE-CYCLE COST OPTIMIZATION OF REINFORCED CONCRETE FRAMES USING METAHEURISTIC ALGORITHMS AND NEURAL NETWORKS

A.R. Taghizadeh and S. Gholizadeh<sup>\*,†</sup>  
*Department of Civil Engineering, Urmia University, Urmia, Iran*

## ABSTRACT

This paper employs a hybrid approach that integrates a metaheuristic algorithm with a properly trained neural network (NN) to perform seismic life-cycle cost optimization of reinforced concrete (RC) frames within the framework of performance-based design. In the proposed hybrid methodology, the center of mass optimization (CMO) metaheuristic algorithm is used to explore the design space. Additionally, a properly trained NN model is employed to estimate the nonlinear seismic response of the RC frames in order to evaluate the design constraints and compute the life-cycle cost during the optimization process within a reasonable computational time. The efficiency of the proposed hybrid methodology is assessed through two performance-based design optimization case studies involving 5- and 10-story RC frames. The numerical results demonstrate that the proposed approach is an effective tool for optimizing the life-cycle cost of RC frames by substantially reducing the computational burden of the optimization process.

**Keywords:** seismic life cycle cost; performance-based design; nonlinear pushover analysis; neural network; reinforced concrete frame.

Received: 2 December 2025; Accepted: 21 January 2026

## 1. INTRODUCTION

Seismic design practice increasingly relies on performance-based design (PBD) [1] to ensure that structures achieve adequate seismic resistance across multiple performance levels. This framework explicitly incorporates nonlinear structural response analyses to quantify potential damage in both structural and nonstructural components. Although this approach provides a more realistic and reliable assessment of seismic performance, it also demands substantially greater computational effort compared with conventional force-based design procedures. As

---

\*Corresponding author: Department of Civil Engineering, Urmia University, Urmia, Iran

†E-mail address: s.gholizadeh@urmia.ac.ir (S. Gholizadeh)

a result, structural engineers face the dual challenge of developing designs that are both cost-efficient and sufficiently reliable to withstand earthquake demands, while also managing the intensive computational requirements inherent to performance-based design methodologies. In recent years, numerous studies have been conducted to address this issue by developing performance-based design optimization techniques [2-6]. These approaches aim to systematically search the design space to identify structural configurations that satisfy prescribed performance objectives while minimizing associated costs. By integrating optimization algorithms with nonlinear structural analysis, researchers have attempted to enhance the efficiency and reliability of seismic design, enabling engineers to achieve improved structural performance and more economical solutions. To account for economic concerns in the design of structures, life-cycle cost analysis can be effectively conducted. In fact, the life-cycle cost of structures is assessed by the initial construction cost and the future seismic damage costs due to earthquakes that can occur during the structure's lifespan [7-8]. Accompanying life-cycle cost analysis by structural optimization techniques offers an efficient technique to design RC frames [9].

Nowadays, metaheuristic algorithms have emerged as an effective and widely adopted solution for solving complex and highly nonlinear optimization problems. These algorithms are typically inspired by stochastic natural phenomena, and their computer implementation is relatively straightforward [10-13]. Despite these advantages, their application to performance-based design optimization often results in a substantial computational burden, primarily due to the large number of nonlinear structural analyses required to evaluate candidate solutions throughout the optimization process. Accurate and efficient evaluation of the seismic performance of structures plays a crucial role in performance-based design optimization. Reliable assessment of seismic behavior is essential for ensuring the safety and functionality of structures. In this context, precise prediction of structural response under seismic loading becomes a key component of the optimization process. Evaluating seismic performance requires careful consideration of several factors, including nonlinear structural behavior, material characteristics, structural configuration, and the intensity and characteristics of expected seismic demands. These aspects significantly influence the accuracy of performance assessment and, consequently, the reliability of the resulting design solutions. However, detailed nonlinear analyses that account for these factors are computationally demanding, particularly when repeated numerous times during an optimization procedure. Therefore, the development of reliable and computationally efficient predictive tools has become an important research direction. Such tools enable rapid estimation of structural responses while maintaining acceptable levels of accuracy, thereby significantly reducing the computational burden of the optimization process. By incorporating these advanced predictive techniques into the design framework, structural engineers can achieve designs that not only satisfy safety and performance requirements but also optimize costs and resource utilization.

In recent years, artificial neural networks have attracted considerable attention as an effective alternative for alleviating the significant computational burden associated with performance-based seismic design and optimization [14]. Owing to their powerful function-approximation capability, neural networks can effectively capture complex and highly nonlinear relationships between input variables and structural responses. This capability makes them particularly suitable for predicting the seismic performance of structures with substantially reduced computational effort compared with conventional nonlinear analysis procedures. By integrating neural network models into the structural design

framework, engineers can obtain accurate predictions of structural responses while significantly decreasing the number of computationally intensive analyses required during the optimization process. In this study, neural network models are employed to estimate the seismic performance of RC frames in terms of the maximum inter-story drift ratios corresponding to the Immediate Occupancy (IO), Life Safety (LS), and Collapse Prevention (CP) performance levels. Specifically, multilayer perceptron (MLP) neural network architectures are adopted to model the complex relationship between structural design variables and seismic response parameters. The developed models consist of multiple hidden layers with varying numbers of neurons in order to investigate different network configurations and identify the architecture that provides the highest prediction accuracy. After training and validating several candidate models, the neural network with the best predictive performance is integrated into the optimization framework. Within this framework, the selected model rapidly predicts the maximum inter-story drift ratios at the specified seismic performance levels. These predictions are then used to evaluate the design constraints and to compute the life-cycle cost of the RC frames, which serves as the objective function of the optimization problem. In this manner, the proposed approach significantly reduces the computational effort required for repeated nonlinear analyses while maintaining reliable estimates of structural seismic performance.

Two representative design cases, a 5-story and a 10-story RC frame, are developed to demonstrate the effectiveness of the proposed methodology. The results show that the approach provides a practical framework for life-cycle optimization of RC frame structures within the PBD framework, highlighting its potential for broader application in real-world engineering practice.

## 2. LIFE-CYCLE COST OF RC FRAMES

Seismic total cost ( $C_T$ ) is a highly valuable indicator for economic decision-making and life-cycle performance assessment of structures. For RC frames,  $C_T$  comprises the initial construction cost ( $C_I$ ) and the life-cycle cost ( $C_{LC}$ ). The initial construction cost of RC frames consists mainly of the costs for concrete, steel, and formwork, which are expressed below.

$$C_I^c = C_C (\sum_i^{nc} b_{c,i} h_{c,i} H_i + \sum_j^{nb} b_{b,j} h_{b,j} L_j) \quad (1)$$

$$C_I^s = C_S (\sum_i^{nc} A_{St,i} H_i + \sum_j^{nb} A_{St,j} L_j) \quad (2)$$

$$C_I^f = C_F (\sum_i^{nc} 2(b_{c,i} + h_{c,i}) H_i + \sum_j^{nb} (b_{b,j} + 2h_{b,j}) L_j) \quad (3)$$

$$C_I = C_I^c + C_I^s + C_I^f \quad (4)$$

where  $C_I^c$  = concrete cost,  $b_{c,i}$  = the width,  $h_{c,i}$  = the depth,  $A_{St,i}$  = steel reinforcement area, and  $H_i$  = the height of the  $i$ th column; Similarly,  $b_{b,j}$  = the width,  $h_{b,j}$  = the depth,  $C_I^s$  = steel reinforcement cost,  $A_{St,j}$  = steel reinforcement area, and  $L_j$  = the length of the  $j$ th beam;  $C_I^f$  = formwork cost;  $nc$  and  $nb$  are the number of columns and beams, respectively; and the unit costs for concrete is  $C_C = 105$  \$/m<sup>3</sup>, for steel reinforcement is  $C_S = 0.9$  \$/kg, and for formwork is  $C_F = 92$  \$/m<sup>2</sup>.

The  $C_{LC}$  encompasses costs related to damage from earthquakes that may occur throughout the structure's lifespan. A cost estimation of this metric requires evaluating structural behavior under a range of seismic intensities. Under the assumptions that seismic events follow a Poisson process and that the structure is returned to its pre-damage condition immediately after each occurrence, Wen and Kang [7-8] proposed a formulation for evaluating life-cycle costs [15]. With this method, the cost corresponding to exceeding each damage state, expressed as a percentage of the initial construction cost, can be determined as follows:

$$C_T = C_I + C_{LC} \quad (5)$$

$$C_{LC} = \frac{1-e^{-\lambda T}}{\lambda} C_I \sum_{i=1}^{nd} MDI_i P_i \quad (6)$$

$$P_i = P(\delta > \delta_i) - P(\delta > \delta_{i+1}) \quad (7)$$

$$P(\delta > \delta_i) = \frac{-1}{T} \ln(1 - \bar{P}(\delta > \delta_i)) \quad (8)$$

$$\bar{P}(\delta > \delta_i) = \gamma \delta_i^{-k} \quad (9)$$

where  $\lambda$  = the annual monetary discount rate and equal to 5%;  $nd$  = the damage states considering to be 7;  $T$  = the structure service life;  $MDI_i$  is mean damage index of  $i$ th damage state as presented in Table 1;  $\delta$  denotes inter-story drift ratio;  $P_i$  denotes the likelihood of exceedance of the  $i$ th damage state in the event of an earthquake;  $P(\delta > \delta_i)$  represents the probability that the maximum inter-story drift ratio exceeds the threshold corresponding to the  $i$ th damage state;  $\bar{P}(\delta > \delta_i)$  denotes the annual probability that the maximum inter-story drift ratio exceeds the threshold of the  $i$ th damage state; the parameters  $\gamma$  and  $k$  are obtained by fitting to known values of  $\bar{P}$  for the seismic hazard levels with exceedance probabilities of 50%, 10%, and 2% over 50 years, along with their corresponding values of  $\delta$  at different performance levels.

Table 1: Damage states, MDI and  $\delta$  for RC frames

| Damage state | Mean damage index | Inter-story drift ratio (%) |
|--------------|-------------------|-----------------------------|
| None         | 0.0               | $\delta \leq 0.1$           |
| Slight       | 0.005             | $0.1 < \delta \leq 0.2$     |
| Light        | 0.05              | $0.2 < \delta \leq 0.4$     |
| Moderate     | 0.2               | $0.4 < \delta \leq 1.0$     |
| Heavy        | 0.45              | $1.0 < \delta \leq 1.8$     |
| Major        | 0.80              | $1.8 < \delta \leq 3.0$     |
| Collapse     | 1.0               | $0.3 < \delta$              |

### 3. SEISMIC OPTIMIZATION OF RC FRAMES

The PBD provisions necessitate that structures satisfy predefined performance levels under specified seismic hazards. This study adopts the IO, LS, and CP performance levels as defined in FEMA 356 and ASCE 41-13 [16]. The corresponding hazard levels are represented by the acceleration response spectra of the frequent, design, and maximum considered earthquakes, which follow Standard No. 2800 [17] and correspond to 50%, 10%, and 2% probabilities of

exceedance in 50 years, respectively.

Nonlinear structural responses are evaluated through pushover analysis, wherein the structure is subjected to a prescribed lateral load pattern until a control point reaches the target displacement. Before analysis, preliminary checks are performed to satisfy geometric, strength, and strong-column-weak-beam requirements in accordance with ACI 318-08 [18]. Additionally, the seismic performance of RC frames is assessed using the design constraints outlined in FEMA 356 and ASCE 41-13, as follows:

$$g_i^D = \frac{\delta^i}{\delta_{all}^i} - 1 \leq 0 ; i = IO, LS, CP \tag{10}$$

$$g_{i,j}^C = \frac{\theta_j^i}{\theta_{all}^{i,c}} - 1 \leq 0 ; i = IO, LS, CP ; j = 1, 2, \dots, nc \tag{11}$$

$$g_{i,j}^B = \frac{\theta_k^i}{\theta_{all}^{i,b}} - 1 \leq 0 ; i = IO, LS, CP ; k = 1, 2, \dots, nb \tag{12}$$

where  $\delta^i$  and  $\delta_{all}^i$  are the maximum inter-story drift and the allowable inter-story drift at  $i$ th performance levels, respectively;  $\theta_j^i$  and  $\theta_k^i$  are the maximum plastic hinge rotation of the  $j$ th column and  $k$ th beam, respectively;  $\theta_{all}^{i,c}$  and  $\theta_{all}^{i,b}$  are the allowable values of the plastic hinge rotation of the column and beam, respectively. According to FEMA 356,  $d_{all}^{IO} = 1\%$ ,  $d_{all}^{LS} = 2\%$ , and  $d_{all}^{CP} = 4\%$ . Also, the allowable plastic rotations of beams and columns at performance levels are determined using Tables 10–7 and 10-8 of ASCE 41–13.

The cross sections of columns and beams serve as design variables during the optimization process of RC frames. In this study, the domain of these variables is the section databases provided in Tables 2 and 3, which are prepared in accordance with ACI 318-08 [18].

Table 2: RC column section database

| No. | Width (mm) | Depth (mm) | Number of D25 bars |
|-----|------------|------------|--------------------|
| 1   | 400        | 400        | 4                  |
| 2   | 400        | 400        | 6                  |
| ⋮   | ⋮          | ⋮          | ⋮                  |
| 51  | 1000       | 1000       | 24                 |
| 52  | 1000       | 1000       | 28                 |

Table 3: RC beam section database

| No. | Width (mm) | Depth (mm) | Number of D22 bars |          |
|-----|------------|------------|--------------------|----------|
|     |            |            | Positive           | Negative |
| 1   | 350        | 400        | 2                  | 2        |
| 2   | 350        | 400        | 3                  | 2        |
| ⋮   | ⋮          | ⋮          | ⋮                  | ⋮        |
| 520 | 400        | 800        | 9                  | 9        |
| 511 | 400        | 800        | 10                 | 10       |

The seismic life-cycle cost optimization problem of RC frames is formulated as follows:

$$\text{Find: } X = \{x_1 \dots x_i \dots x_{nb+nc}\}^T \quad (13)$$

$$\text{To minimize: } C_T(X) \quad (14)$$

$$\text{Sobjec to: } g_l(X) \leq 0, l = 1, 2, \dots, n \quad (15)$$

where  $X$  is a vector of design variables;  $x_i$  is the design variable of the  $i$ th element group;  $g_l$  is the  $l$ th design constraint; and  $n$  is the number of design constraints.

This paper employs the exterior penalty function method (EPFM) [19] to handle the design constraints, with the pseudo-unconstrained objective function expressed as follows:

$$\Phi(X) = C_T(X) \left( 1 + r_p \sum_{l=1}^n (\max\{0, g_l(X)\}) \right) \quad (16)$$

where  $\Phi$  is the pseudo-unconstrained objective function, and  $r_p$  is the penalty parameter.

#### 4. CENTER OF MASS OPTIMIZATION ALGORITHM

Center of mass optimization (CMO) [20] is based on the concept of center of mass in physics. In the CMO algorithm, a population of  $np$  randomly selected particles ( $X_i, i \in [1, np]$ ) is generated in the design space. The mass of the  $i$ th particle  $m_i$  is determined as follows:

$$m_i = \frac{1}{f(X_i)} \quad (17)$$

Particles are sorted in ascending order of mass and then evenly divided into two groups, G1 and G2, where the first half forms G1 and the remainder forms G2. Each particle in G1 is paired with its counterpart in G2. The particles in G1 are paired with their corresponding ones in G2. For the  $j$ th pair ( $j=1, \dots, np/2$ ) at iteration  $t$ , the center of mass and the distance between the particles are determined as follows:

$$X_j^c(t) = \frac{m_j X_j(t) + m_{j+\frac{np}{2}} X_{j+\frac{np}{2}}(t)}{m_j + m_{j+\frac{np}{2}}} \quad (18)$$

$$d_j(t) = \left| X_j(t) - X_{j+\frac{np}{2}}(t) \right| \quad (19)$$

To switch between exploration and exploitation of the CMO, the following control parameter ( $CP$ ) is computed, where  $t_{max}$  is the maximum number of iterations.

$$CP(t) = \exp\left(-\frac{5t}{t_{max}}\right) \quad (20)$$

The position of the  $j$ th couple of particles is updated using the following equations

$$\text{if } d_j(t) > CP(t) \quad (21)$$

$$X_j(t+1) = X_j(t) - R_1 \left( X_j^C(t) - X_j(t) \right) + R_2 \left( X_b - X_j(t) \right) \quad (22)$$

$$X_{j+\frac{np}{2}}(t+1) = X_{j+\frac{np}{2}}(t) - R_3 \left( X_j^C(t) - X_{j+\frac{np}{2}}(t) \right) + R_4 \left( X_b - X_{j+\frac{np}{2}}(t) \right) \quad (23)$$

$$\text{if } d_j(t) \leq CP(t) \quad (24)$$

$$X_j(t+1) = X_j(t) + R_5 \left( X_j^C(t) - X_{j+\frac{np}{2}}(t) \right) \quad (25)$$

$$X_{j+\frac{np}{2}}(t+1) = X_{j+\frac{np}{2}}(t) + R_6 \left( X_j^C(t) - X_{j+\frac{np}{2}}(t) \right) \quad (26)$$

where  $R_1$  to  $R_6$  are vectors of random numbers in  $[0,1]$ ; and  $X_b$  is the best solution found.

There is a mutation operator in CMO to decrease the probability of local optima entrapment. A mutation rate  $mr = 0.2$  is taken, and in iteration  $t$ , a number between 0 and 1 is randomly selected for each particle in group G1 ( $X_j, j=1, \dots, np/2$ ).

$$r_j(t) \in [0, 1] \quad (27)$$

$$X_j(t) = \{x_{j1}(t) \quad x_{j2}(t) \quad \dots \quad x_{ji}(t) \quad \dots \quad x_{jm}(t)\}^T \quad (28)$$

For  $j$ th particle, if the selected random number is less than the mutation rate, one randomly selected component will be regenerated in the design space as follows

$$\text{if } r_j(t) \leq mr \rightarrow x_{ji}(t) = x_{ji}^L + \mu(t) \times (x_{ji}^U - x_{ji}^L) \quad (29)$$

where  $\mu$  is a random number in the interval  $[0, 1]$  in iteration  $t$ ; and  $x_{ij}^L$  and  $x_{ij}^U$  are lower and upper bounds of  $x_{ji}$  in design space.

## 5. MULTILAYER PERCEPTRON

Nowadays, neural network models offer an efficient means of tackling complex, computationally demanding problems. Their widespread adoption stems from an ability to learn from data and prior experiences. A key benefit of a properly trained model lies in its capacity to deliver approximate solutions with a significantly lower computational cost. Such approximations prove especially valuable when obtaining exact responses requires intensive calculations and rapid estimates are essential. In these scenarios, a neural network model is trained on data generated through a series of analyses. These analyses yield data that are subsequently processed into input-target pairs, forming the basis for training. In this work, a multilayer perceptron (MLP) model is employed, trained using the back-propagation (BP) gradient-based minimization algorithm [21]. As illustrated in Fig. 1, the MLP consists of multiple hidden layers and a single output layer, with the tangent sigmoid function employed as the transfer function for the hidden-layer neurons.

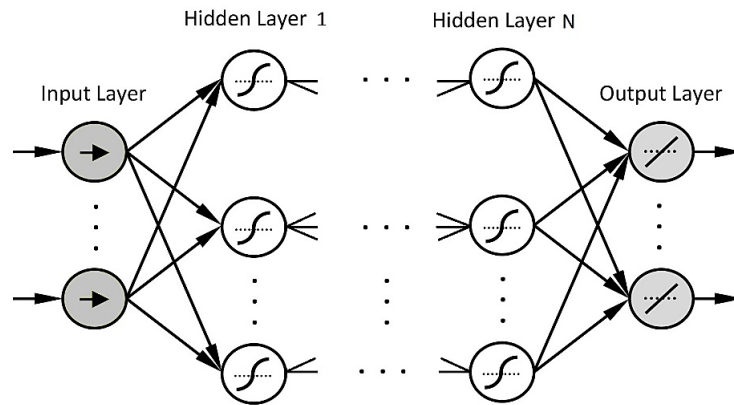


Figure 1: Architecture of the MLP model

The training algorithm of the BP model is a gradient-descent optimization that adjusts the weights along the steepest-descent direction. The BP technique uses the Levenberg-Marquardt (LM) [21] algorithm to approach second-order training speed without having to compute the Hessian matrix. Moreover, this paper utilizes the regularization technique [21] to prevent overfitting.

Previous studies [9, 14] have demonstrated that, in the seismic optimization of RC frames, the constraints related to the maximum inter-story drift ratio are the most critical. As a result, the satisfaction of these constraints guarantees the feasibility of the obtained optimal designs. Consequently, in this a MLP model is trained to predict the maximum inter-story drift ratios at the IO, LS, and CP seismic performance levels for RC frames. The model is developed to capture the nonlinear relationship between the structural design variables ( $X$ ), as inputs, and the resulting maximum inter-story drift ratios at the IO, LS, and CP seismic performance levels as the outputs ( $\delta^i$ ;  $i = \text{IO, LS, CP}$ ). Figure 3 illustrates the flowchart of the training and testing for the MLP model. In which, Percentage Error (PE), Mean Absolute Percentage Error (MAPE), and Root Mean Square Error (RMSE) are used as the evaluation metrics.



Figure 2: Flowchart of training and testing of the MLP model

## 6. NUMERICAL EXAMPLES

Two design examples of 5- and 10-story RC frames are presented to demonstrate the effectiveness of the proposed methodology. The member grouping details of these frames are illustrated in Fig. 3. A uniformly distributed dead load of 24.42 kN/m and a live load of 11.768 kN/m are applied to all beams. Concrete with a cylindrical compressive strength of 28 MPa and a modulus of elasticity of 25,044 MPa is considered in the analysis. The reinforcing steel bars are assumed to have a yield stress of 420 MPa and a modulus of elasticity of 210 GPa.



Figure 3: 5 and 10-story RC frames

For each design example, an MLP model is trained to predict the maximum inter-story drift ratios corresponding to the specified seismic performance levels. The trained model is subsequently integrated into the PBD optimization process of the RC frames. To evaluate the effectiveness of the MLP-based optimization process, 50 independent optimization runs are conducted using the CMO algorithm.

### 6.1. First example: 5-story RC frame

In this example, 500 samples are generated and used for training and testing the MLP model to predict the maximum inter-story drift ratios of the 5-story RC frame. For the best-performing model, which consists of three hidden layers with six neurons in each layer, the MAPE and RMSE in training and testing phases for predicting  $\delta^{IO}$ ,  $\delta^{LS}$ , and  $\delta^{CP}$  are presented in Table 4. Additionally, the absolute percentage of error (APE) is shown in Fig 4. These results demonstrate the acceptable accuracy of the MLP.

Table 4: Evaluation metrics for MLP trained for the 5-story RC frame

| Seismic Response | Training |      | Testing |      |
|------------------|----------|------|---------|------|
|                  | MAPE     | RMSE | MAPE    | RMSE |
| $\delta^{IO}$    | 12.25    | 0.11 | 13.25   | 0.14 |
| $\delta^{LS}$    | 8.15     | 0.12 | 9.15    | 0.15 |
| $\delta^{CP}$    | 6.05     | 0.13 | 7.05    | 0.16 |

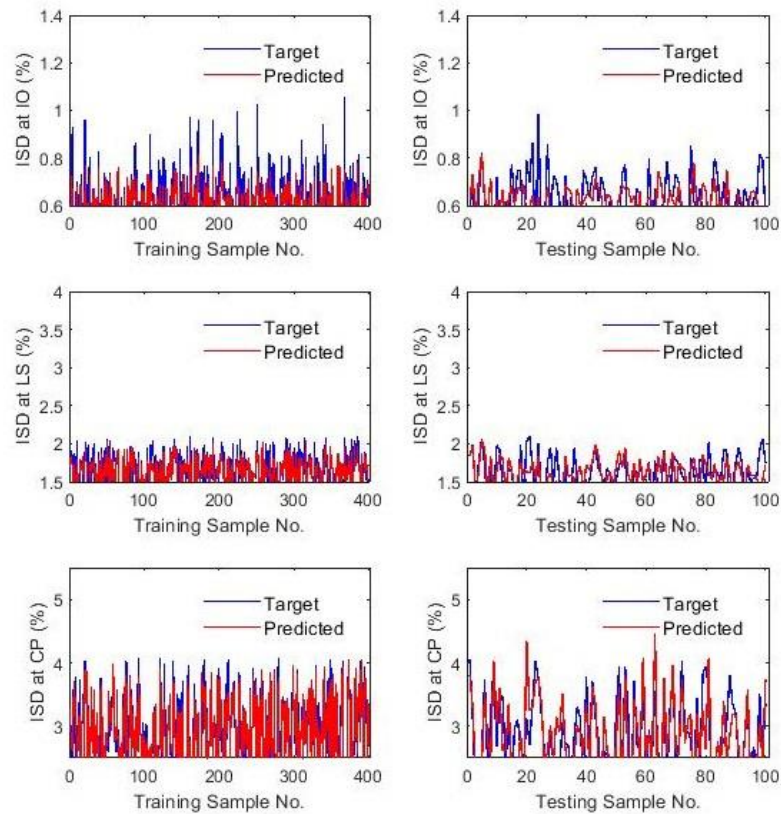


Figure 4: APE of the MLP for predicting the inter-story drift (ISD) of the 5-story RC frame

Table 5 presents the two best designs obtained for the 5-story RC frame from 50 independent optimization runs. In the optimization process, an initial population of 50 particles is employed over 50 iterations. Nonlinear pushover analyses are performed for the best designs, and the resulting structural responses are compared with the predictions of the trained MLP model in Table 6 in order to demonstrate the acceptable prediction accuracy of the model.

Table 5: The best designs of the 5-story RC frame

| Variables | Design I  |       |                |          | Design II |       |                |          |
|-----------|-----------|-------|----------------|----------|-----------|-------|----------------|----------|
|           | Dim. (mm) |       | Number of bars |          | Dim. (mm) |       | Number of bars |          |
|           | Width     | Depth | Positive       | Negative | Width     | Depth | Positive       | Negative |
| C1        | 600       | 600   | 6              | 6        | 700       | 700   | 8              | 8        |
| C2        | 600       | 600   | 6              | 6        | 550       | 550   | 5              | 5        |
| C3        | 550       | 550   | 6              | 6        | 550       | 550   | 4              | 4        |
| C4        | 550       | 550   | 5              | 5        | 450       | 450   | 4              | 4        |
| C5        | 500       | 500   | 4              | 4        | 400       | 400   | 3              | 3        |
| B1        | 400       | 750   | 3              | 3        | 400       | 700   | 4              | 4        |
| B2        | 400       | 650   | 4              | 4        | 400       | 700   | 3              | 3        |
| B3        | 350       | 600   | 4              | 4        | 400       | 650   | 4              | 4        |
| B4        | 300       | 550   | 4              | 4        | 400       | 600   | 4              | 4        |
| B5        | 300       | 500   | 2              | 2        | 300       | 600   | 2              | 2        |

Table 6: Accurate and predicted responses of the best designs of the 5-story RC frame

| Results           | Design I |          | Design II |          |
|-------------------|----------|----------|-----------|----------|
|                   | Pushover | MLP      | Pushover  | MLP      |
| $C_I$ (\$)        | 31614.57 | 31614.57 | 31370.62  | 31370.62 |
| $C_{LC}$ (\$)     | 23185.32 | 23921.63 | 23283.76  | 23643.75 |
| $C_T$ (\$)        | 54799.88 | 55536.20 | 54654.37  | 55014.37 |
| $\delta^{IO}$ (%) | 0.7      | 0.67     | 0.63      | 0.65     |
| $\delta^{LS}$ (%) | 1.8      | 1.99     | 1.94      | 1.96     |
| $\delta^{CP}$ (%) | 2.9      | 3.09     | 3.1       | 3.18     |

Comparison of the results obtained from pushover analysis and the MLP model shows that the differences in life cycle costs and maximum inter-story drifts are less than 3% and 10%, respectively, while the computational effort of the optimization is significantly reduced.

6.2 Second example: 10-story RC frame

An MLP model is trained and tested using 800 generated samples to predict the seismic response of the 10-story RC frame.

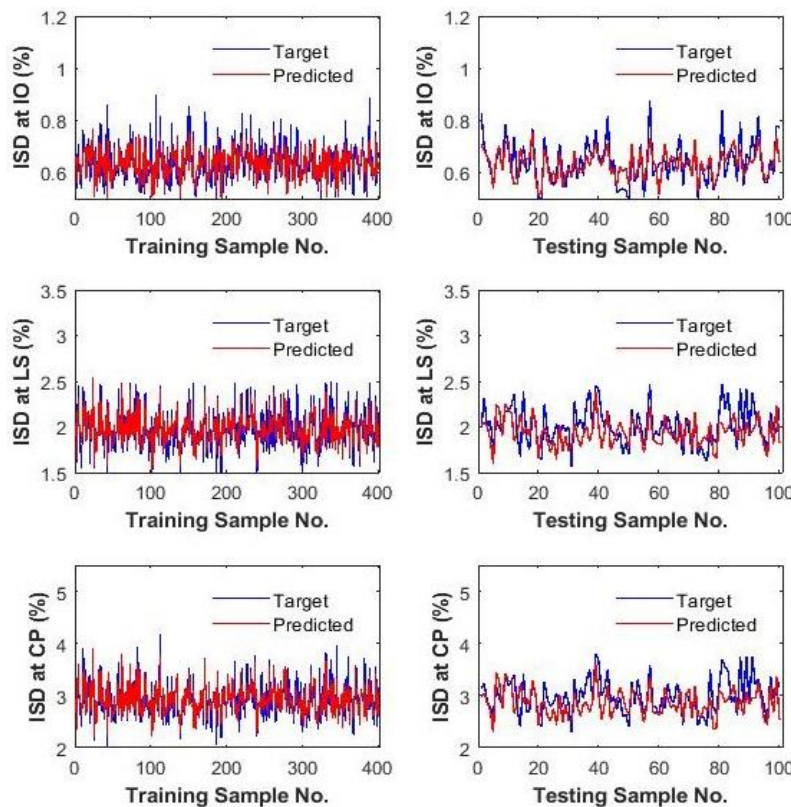


Figure 5: APE of the MLP for predicting the inter-story drift (ISD) of the 10-story RC frame

For the best-performing model, which consists of three hidden layers with six neurons in each layer, the APE in training and testing phases is shown in Fig. 5. Moreover, Table 7 presents the MAPE and RMSE in training and testing phases for predicting the seismic

response. These results confirm the MLP's acceptable accuracy, supporting its integration into the optimization process.

Table 7: Evaluation metrics for MLP trained for the 10-story RC frame

| Seismic Response | Training |      | Testing |      |
|------------------|----------|------|---------|------|
|                  | MAPE     | RMSE | MAPE    | RMSE |
| $\delta^{IO}$    | 5.47     | 0.04 | 6.45    | 0.05 |
| $\delta^{LS}$    | 5.33     | 0.13 | 8.09    | 0.21 |
| $\delta^{CP}$    | 5.21     | 0.19 | 8.70    | 0.34 |

Table 8 lists the two optimal designs for the 10-story RC frame, obtained from 50 independent optimization runs. Each run used a population of 50 particles over 100 iterations. To validate the MLP model's prediction accuracy, nonlinear pushover analyses were performed on the best designs, and the resulting structural responses are compared against the model's predictions in Table 9.

Table 8: The best designs of the 10-story RC frame

| Variables | Design I  |       |                |          | Design II |       |                |          |
|-----------|-----------|-------|----------------|----------|-----------|-------|----------------|----------|
|           | Dim. (mm) |       | Number of bars |          | Dim. (mm) |       | Number of bars |          |
|           | Width     | Depth | Positive       | Negative | Width     | Depth | Positive       | Negative |
| C1        | 950       | 950   | 12             | 12       | 800       | 800   | 11             | 11       |
| C2        | 750       | 750   | 9              | 9        | 800       | 800   | 11             | 11       |
| C3        | 650       | 650   | 9              | 9        | 750       | 750   | 10             | 10       |
| C4        | 600       | 600   | 7              | 7        | 650       | 650   | 8              | 8        |
| C5        | 500       | 500   | 6              | 6        | 550       | 550   | 7              | 7        |
| B1        | 400       | 800   | 6              | 6        | 400       | 800   | 6              | 6        |
| B2        | 400       | 750   | 7              | 7        | 400       | 700   | 7              | 7        |
| B3        | 400       | 650   | 8              | 8        | 400       | 650   | 8              | 8        |
| B4        | 400       | 650   | 6              | 6        | 400       | 650   | 6              | 6        |
| B5        | 300       | 600   | 5              | 5        | 300       | 600   | 5              | 5        |

Table 9: Accurate and predicted responses of the best designs of the 10-story RC frame

| Results           | Design I  |           | Design II |           |
|-------------------|-----------|-----------|-----------|-----------|
|                   | Pushover  | MLP       | Pushover  | MLP       |
| $C_I$ (\$)        | 103364.68 | 103364.68 | 105214.65 | 105214.65 |
| $C_{LC}$ (\$)     | 74644.78  | 71666.13  | 72855.57  | 75623.25  |
| $C_T$ (\$)        | 178009.46 | 175030.81 | 178070.22 | 180837.9  |
| $\delta^{IO}$ (%) | 0.63      | 0.58      | 0.57      | 0.59      |
| $\delta^{LS}$ (%) | 1.86      | 1.83      | 1.94      | 1.74      |
| $\delta^{CP}$ (%) | 2.91      | 2.72      | 2.77      | 2.57      |

Comparing pushover analysis results with the MLP model predictions reveals differences below 5% for life-cycle costs and below 10% for maximum inter-story drifts, all while substantially reducing the optimization's computational effort.

## 7. CONCLUSIONS

This study proposed a hybrid performance-based design optimization framework that integrates the CMO metaheuristic with a properly trained MLP neural network to minimize the seismic life-cycle cost of RC frames. The effectiveness of the methodology was demonstrated through two case studies involving 5-story and 10-story RC frames. The following conclusions are drawn:

In both examples, the trained MLP models exhibited acceptable accuracy in predicting maximum inter-story drift ratios at different seismic performance levels. For the 5-story frame, MAPE and RMSE values confirmed the model's reliability, for the 10-story frame, similar metrics validated its performance. For the optimal designs obtained from 50 independent optimization runs, the life-cycle costs predicted by the MLP model differed from pushover analysis results by less than 3% (5-story frame) and less than 5% (10-story frame). Maximum inter-story drift differences remained below 10% for both frames. This level of agreement confirms that the MLP model captures the essential nonlinear seismic response with sufficient engineering accuracy. By replacing computationally expensive nonlinear pushover analyses with rapid MLP predictions, the proposed hybrid framework dramatically reduced the computational burden of the optimization process. This efficiency enables extensive design-space exploration (e.g., 50 independent runs) that would be impractical with conventional analysis methods. The successful application to both a 5-story and a 10-story RC frame demonstrates the scalability and robustness of the hybrid CMO-MLP approach. The methodology is not limited to low-rise structures and can be extended to taller frames with appropriate sample generation and model training.

In summary, the hybrid metaheuristic-neural network approach presented in this paper is an effective and efficient solution for performance-based seismic optimization of RC frames.

## REFERENCES

1. FEMA-356, *Prestandard and Commentary for the Seismic Rehabilitation of Buildings*. Federal Emergency Management Agency, Washington DC, 2000.
2. Kaveh A, Zakian P. Performance based optimal seismic design of RC shear walls incorporating soil–structure interaction using CSS algorithm. *Int J Optim Civil Eng* 2012; **2**: 383–405.
3. Ganjavi B, Hajirasouliha I. Optimum performance-based design of concentrically braced steel frames subjected to near-fault ground motion excitations. *Int J Optim Civil Eng* 2019; **9**:177–193.
4. Gholizadeh S, Hasançebi O. Efficient neural network-aided seismic life-cycle cost optimization of steel moment frames. *Comput Struct* 2024;**301**:107443.
5. Gholizadeh S, Hasançebi O, Eser H, Koçkaya O. Seismic collapse safety based optimization of steel Moment-Resisting frames. *Structures* 2022;**237**:112207.
6. Ghaderi M, Gholizadeh S. Mainshock-aftershock low-cycle fatigue damage evaluation of performance-based optimally designed steel moment frames. *Eng Struct* 2021;**237**:112207.
7. Wen YK, Kang YJ. Minimum building life-cycle cost design criteria. I: Methodology. *J Struct Eng* 2001;**127**:330-37.

8. Wen YK, Kang YJ. Minimum building life-cycle cost design criteria. II: Applications, *J Struct Eng* 2001;**127**:338-46.
9. Razavi N, Gholizadeh S. Seismic collapse safety analysis of performance-based optimally designed reinforced concrete frames considering life-cycle cost. *J Build Eng* 2021;**44**:103430.
10. Kaveh A. Applications of artificial neural networks and machine learning in civil engineering, studies in Computational Intelligence 1168, Springer, 2024.
11. Kaveh A, Talatahari S. An enhanced charged system search for configuration optimization using the concept of fields of forces. *Struct Multidiscip Optim*, 2011;**43**:339-351.
12. Kaveh A. Advances in metaheuristic algorithms for optimal design of structures, Springer International Publishing, Switzerland, 3rd edition, 2021.
13. Bigham A, Gholizadeh S. Topology optimization of nonlinear single-layer domes by an improved electro-search algorithm and its performance analysis using statistical tests. *Struct Multidiscip Optim* 2020;**62**:1821-48.
14. Razavi N, Gholizadeh S, Hasançebi O. Optimal seismic design of reinforced concrete moment-resisting frames using an improved metaheuristic and neural networks. *Structures* 2025;**73**:108464.
15. Mitropoulou CC, Lagaros ND, Papadrakakis M. Life-cycle cost assessment of optimally designed reinforced concrete buildings under seismic actions. *Reliab Eng Syst Safe* 2011;**96**:1311-31.
16. ASCE 41-13. Seismic Evaluation and Retrofit of Existing Buildings, American Society of Civil Engineers, Reston (VA), 2014.
17. Standard No. 2800. Iranian Code of Practice for Seismic Resistant Design of Buildings, Building and Housing Research Center, Tehran, 2014.
18. ACI 318-08. Building Code Requirements for Structural Concrete and Commentary, American Concrete Institute, Farmington Hills, MI, 2008.
19. Vanderplaats GN. *Numerical Optimization Techniques for Engineering Design: With Application*, McGraw-Hill, NewYork, 1984.
20. Gholizadeh S, Ebadijalal M. Performance based discrete topology optimization of steel braced frames by a new metaheuristic. *Adv Eng Softw* 2018; **123**: 77–92.
21. Hagan MT, Demuth HB, Beal MH. Neural network design, PWS Publishing Company, Boston, 1996.